Science of the Total Environment 934 (2024) 173260

Contents lists available at ScienceDirect

Science of the Total Environment

journal homepage: www.elsevier.com/locate/scitotenv

# Sustainable lindane waste remediation: Surfactant-driven residual DNAPL extraction and oxidation in a real landfill (LIFE SURFING)

Jesús Fernández [b], David Lorenzo [a], Jorge Net [b], Elena Cano [b], Patricia Saez [a], Carlos Herranz [c], Carmen M. Domínguez [a], Salvador Cotillas [a], Aurora Santos [a,*]

[a] Chemical Engineering and Materials Department, University Complutense of Madrid, Spain
[b] Department of Environment and Tourism, Government of Aragon, Spain
[c] Sociedad Aragonesa de Gestión Agroambiental SARGA, Zaragoza, Spain

## HIGHLIGHTS

- SEAR and S-ISCO were successfully implemented at Bailin Landfill.
- About 130 kg of DNAPL were removed in SEAR and 20 kg in S-ISCO.
- Low levels of toxic compounds in groundwater were maintained after S-ISCO.
- Innovative barrier zone strategy was implemented avoiding the pollutant dispersion.

## GRAPHICAL ABSTRACT

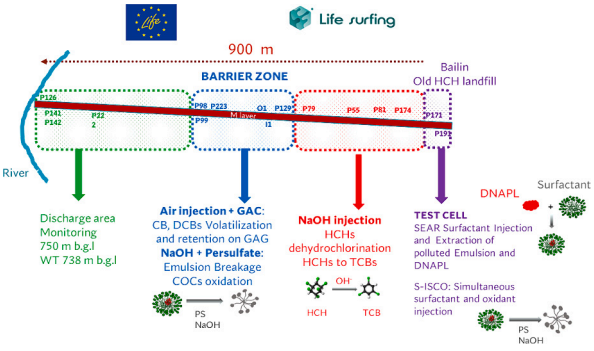


## ARTICLE INFO

*Keywords:*
DNAPL
SEAR
S-ISCO
Lindane
Fractured landfill
LIFE SURFING

## ABSTRACT

The LIFE SURFING Project was carried out at the Bailin Landfill in Sabiñánigo, Spain (2020-2022), applying Surfactant Enhanced Aquifer Remediation (SEAR) and In Situ Chemical Oxidation (S-ISCO) in a 60-meter test cell beneath the old landfill, to remediate a contaminated aquifer with dense non-aqueous phase liquid (DNAPL) from nearby lindane production. The project overcame traditional extraction limitations, successfully preventing groundwater pollution from reaching the river.

In spring 2022, two SEAR interventions involved the injection of 9.3 $m^3$ (SEAR-1) and 6 $m^3$ (SEAR-2) of aqueous solutions containing 20 g/L of the non-ionic surfactant *E*-Mulse 3®, with bromide (around 150 mg/L) serving as a conservative tracer. 7.1 and 6.0 $m^3$ were extracted in SEAR-1 and SEAR-2, respectively, recovered 60–70 % of the injected bromide and 30–40 % of the surfactant, confirming surfactant adsorption by the soil. Approximately 130 kg of DNAPL were removed, with over 90 % mobilized and 10 % solubilized. A surfactant-to-DNAPL recovery mass ratio of 2.6 was obtained, a successful value for a fractured aquifer. In September 2022, the S-ISCO phase entailed injecting 22 $m^3$ of a solution containing persulfate (40 g/L), *E*-Mulse 3® (4 g/L), and NaOH (8.75 g/L) in pulses over 48 h, oxidizing around 20 kg of DNAPL and ensuring low toxicity levels after that.

* Corresponding author.
*E-mail address:* aursan@ucm.es (A. Santos).

https://doi.org/10.1016/j.scitotenv.2024.173260
Received 26 December 2023; Received in revised form 10 May 2024; Accepted 13 May 2024
Available online 16 May 2024

Preceding the SEAR and S-ISCO trials, 2020 and 2021 were dedicated to detailed groundwater flow characterizations, including hydrological and tracer studies. These preliminary investigations allowed the design of a barrier zone between 317 and 557 m from the test cell and the river, situated 900 m away. This zone, integrating alkali dosing, aeration, vapor extraction, and oxidant injection, effectively prevented the escape of fluids to the river. Neither surfactants nor contaminants were detected in river waters post-treatment. The absence of residual phase in test cell wells and reduction of chlorinated compound levels in groundwater were noticed till one year after S-ISCO.

## 1. Introduction

Remediating hydrophobic organic contaminants (HOCs) in soil and groundwater presents substantial challenges due to their low solubility (Trellu et al., 2016). Accidental releases or intentional dumping of organic liquid phases result in persistent Non-Aqueous Phase Liquids (NAPLs), leading to continuous groundwater contamination (Liu et al., 2021; Tomlinson et al., 2017). Methods such as "pump and treat" or In Situ Chemical Oxidation (ISCO) face limitations in treating polluted sites with NAPL due to low solubility and hindered contact between organic and aqueous phases (Akyol, 2018; Siegrist et al., 2011; Stroo et al., 2012; Tressler and Uchrin, 2014). Moreover, trapped residues in soil pores or fractures persist for decades, causing contamination in groundwater plumes. Dense NAPLs (DNAPLs), composed of industrial solvents and chlorinated compounds, pose exceptionally high environmental risks due to their high toxicity (CLU-IN, 1991; Wang et al., 2023b).

Soil Flushing treatments like SEAR or SER, involving surfactant injection, have gained attention for their ability to solubilize and mobilize DNAPLs (Abriola et al., 2012; Barbati et al., 2023; Cheng et al., 2017; Guadaño et al., 2022; Huo et al., 2020; Liu et al., 2021; Maire et al., 2018; McCray et al., 2011; Saint-Fort, 2022). These treatments inject an aqueous surfactant solution into the contaminated zone, enhancing solubilization and decreasing interfacial tension between organic and aqueous phases. This promotes the mobilization of the organic phase and the solubilization of Contaminants of Concern (COCs) (Kang et al., 2019; Mo et al., 2024; Pennell et al., 2014; Wang et al., 2023a). After a required contact time, polluted emulsions and mobilized organic phases are extracted and managed on-site (Dominguez et al., 2019; Sánchez-Yepes et al., 2024).

Confining injected fluids to the contaminated area in SEAR is vital to prevent pollutant dispersion (Abriola et al., 2012; Cheng et al., 2017; Londergan and Yeh, 2003). The technology must capture solubilized contaminants, and extracted polluted emulsions must be managed appropriately (Dominguez et al., 2019). While understanding fluid transport is essential, most studies have been conducted in controlled environments, with few in real contaminated sites (Guadaño et al., 2022; Wang et al., 2023b).

Simultaneous injection of oxidants and surfactants (S-ISCO) is a promising technology (Besha et al., 2018). The surfactant enhances solubility and improves oxidation rates but competes with contaminants for oxidants (García-Cervilla et al., 2021). This competition may lead to unproductive oxidant consumption by surfactants, reducing solubility. The concentration of surfactants influences micelle aggregation structures, impacting reactivity against oxidants and solubilized contaminants. S-ISCO application does not require fluid extraction, but establishing sufficient contact time between oxidants and contaminants in the micelles is crucial to ensure effective oxidation and emulsion breakage before reaching superficial waters or posing environmental risks (Akyol, 2018; Demiray et al., 2023; Garcia-Cervilla et al., 2022a; Herzog et al., 2023; Sun et al., 2021; Wei et al., 2022; Xu et al., 2024).

The SEAR and S-ISCO technologies have been employed in the LIFE SURFING project to address the liquid wastes generated from Lindane production disposed of in the Bailin landfill, which are still confined within fractures in the landfill.

Lindane (gamma-hexachlorocyclohexane, gamma-HCH) was used as a broad-spectrum pesticide during the second half of the 20th century. It was manufactured by benzene photochlorination, yielding a mixture of isomers (alpha-, beta-, gamma-, delta-, epsilon-HCH) known as technical HCH. Gamma-HCH is the only isomer with insecticidal properties, and the HCHs mixture requires purification by distillation with solvents and fractional crystallization. This process was highly inefficient, and for each tonne of Lindane, approximately 6–10 t of other HCH isomers were generated. Solid and liquid wastes from lindane production were usually dumped near the production sites, resulting in significant soil and groundwater pollution (Vijgen et al., 2019; Vijgen et al., 2022). Due to its danger, the production and use of Lindane were banned in most countries. Nevertheless, there are many HCH-polluted spots around the world requiring urgent remedial actions. One particular case is that of Sabiñánigo (Huesca, Spain), where the company INQUINOSA dumped >140,000 t of HCH waste in two unlined landfills: Sardas and Bailín (Fernandez et al., 2013). Residues included solid (HCH isomers) and liquid wastes. The liquid waste, originating from unsuccessful dechlorination reactions, distillation tails, and residual solvents, forms a dense non-aqueous phase liquid (DNAPL). This DNAPL is a complex mixture of 28 chlorinated organic compounds (COCs), including chlorobenzenes, HCHs, and HeptaChlorocycloHexanes (HeptaCHs) (Santos et al., 2018a). The hydrophobic nature of this mixture generally intensifies with the chlorine content of the molecules. Due to their toxicity and environmental persistence, some of the components have been included in the Stockholm Convention list of persistent organic pollutants (Vijgen et al., 2011).

With a density ranging from approximately 1.5 to 1.8 g/mL, the DNAPL migrates through the subsurface until it encounters an impermeable layer. Along its path, the DNAPL is adsorbed and trapped in the pores of soil particles with small particle sizes or soil fractures, leading to subsoil contamination and groundwater.

The Bailin landfill was located on a vertical alternation of sandstone and siltstone, with different degrees of fracturing. At depths below 10 m b.g.l., fracturing affects only the sandstone layers, generating a series of isolated aquifers that flow in the direction of the layers towards the Gállego River, with the sandstone layer M under the landfill well connected with the Gallego River (Fig. 1). The dumped DNAPL in the old landfill was retained in the fractures of the sandstone layer M, resulting in a plume of highly contaminated groundwater downstream with the associated risk for the Gallego river and the population.

In 2004, this DNAPL was detected, its dispersion was delimited, and its pneumatic pumping and external waste management began (Fernandez et al., 2013). After 16 years of pneumatic pumping, the dense phase (DNAPL) in the Bailín landfill aquifer is physically inefficient to extract, making it necessary to apply advanced techniques to remove the residual DNAPL and, consequently, achieve the reduction of chlorinated compounds in groundwater (Fig. SM-1). The removal of this residual DNAPL should also prevent possible groundwater pollution rebounds in the future.

Surfactant Enhanced Aquifer Remediation (SEAR) and In Situ Chemical Oxidation enhanced by Surfactant addition (S-ISCO) have been proposed and tested in the Bailin Landfill (Sabiñanigo, Spain) through the Life SURFING project: "SURFactant enhanced chemical oxidation for remediating DNAPL" (EU LIFE Program LIFE17 ENV/ES/000260, https://lifesurfing.eu/). The pilot test was carried out in a test cell of 60 m in length, located in the old landfill (the most contaminated area). Fluids (surfactants in SEAR or surfactants and oxidants in S-ISCO)

were injected (and extracted in SEAR).

Previous works were carried out to select the oxidant and surfactant most suitable for landfill lithology and DNAPL compositions. Sodium Persulfate was used as an oxidant, and sodium hydroxide was the activator selected, with this system successfully applied in previous studies for chlorobenzenes (Santos et al., 2018b). Moreover, as the oxidation of COCs was carried out in energic alkaline conditions, dehydrochlorination reactions of pentachlorocyclohexene (PentaCXs) and hexachlorocyclohexane (HCHs) isomers to trichlorobenzene isomers (TCBs), and hexachlorocyclohexane (HexaCXs) and heptachlorocyclohexane isomers (HeptaCHs) to tetrachlorobenzenes (TetraCBs) were found in the aqueous phase in the absence and presence of surfactants (Garcia-Cervilla et al., 2022a) (Fig. SM-2).

The surfactant selected was *E*-Mulse 3 ® supplied by EthicalChem. This biodegradable polyethoxylated surfactant showed high solubilization of DNAPL found at Bailin Landfill at neutral and alkaline pH (García-Cervilla et al., 2020). Moreover, this surfactant allowed an adequate balance between the surfactant oxidation (unproductive consumption of oxidant and surfactant) and the oxidation of DNAPL solubilized in the micelles (Garcia-Cervilla et al., 2022a; García-Cervilla et al., 2021).

Management of polluted emulsion was studied by selective oxidation of COCs in the emulsion (Dominguez et al., 2019), by selective adsorption of COCs in GAC and further adsorbent regeneration (Sánchez-Yepes et al., 2024), or by alkalization of the emulsion with COCs volatilization in an air stream enhanced by temperature and retention of COCs in the gas phase in GAC (Sáez et al., 2022).

A pilot test injecting surfactant and oxidants (SEAR and S-ISCO events) was conducted in a test cell at the Bailin Landfill. The DNAPL spill occurred decades ago in this area, so the subsurface and groundwater are heavily contaminated. Hydrogeological and tracer tests were carried out during 2020 and 2021 to determine the groundwater flow when fluids were injected into the test cell and the required control actions downstream before reaching the Gallego River (about 900 m from the test cell). DNAPL extracted in SEAR (solubilized and mobilized) and DNAPL oxidized in the S-ISCO event have been determined, and the removal DNAPL rate was compared with that obtained with a pneumatic pump.

Despite the relatively high number of studies on the application of SEAR (Surfactant Enhanced Aquifer Remediation) in soil remediation, the majority of these investigations have been conducted in laboratory settings, using either batch or soil column experiments, and significantly fewer studies have been carried out at a full-scale level. Furthermore, in the case of fractured media, there are no real-scale application data for the use of surfactants to remove residual DNAPL (Dense Non-Aqueous Phase Liquid). However, the behaviour of these fractured media will be completely different from that found in granular media (Guadaño et al., 2022). Although the surfactant for this DNAPL removal was selected in the laboratory using soil from an alluvial source (Garcia-Cervilla et al., 2021), its application to a real-scale fractured medium has not been studied. The adsorption of surfactants in fractures and the contact time required to achieve solubilization equilibrium may substantially differ from what is observed in the laboratory (García-Cervilla et al., 2020). Additionally, the dispersion of the surfactant and contaminants not extracted, which escape through the fractures, and the control of the contamination plume that leaks downstream are phenomena that need to be studied as they are critical for its implementation at field scale.

When surfactants and oxidants are simultaneously injected, known as S-ISCO, the body of scientific literature is much smaller and almost entirely conducted in laboratory settings. There are no studies on their application in fractured media. This study utilizes the surfactant and oxidant concentrations selected in the laboratory for this DNAPL (Garcia-Cervilla et al., 2022a; García-Cervilla et al., 2021). However, the application in fractured media requires injection strategies that consider the reaction kinetics in the aqueous phase, to ensure sufficient contact time to remove contaminants and control of dispersion. These aspects are analyzed in this study.

Therefore, this study provides valuable and novel scientific-technical information for the application of processes with surfactants and surfactant-oxidants in real fractured media and with aged residual contamination that cannot be extracted by traditional pumping.

## 2. Materials and methods

### 2.1. Chemicals

The surfactant selected was *E*-Mulse-3 ® (E3), supplied by EthicalChem. This surfactant is formulated with limonene as co-solvent (15–25 % in weight). Sodium persulfate (PS, provided by SIMARSA) was used as an oxidant, and sodium hydroxide (NaOH, SIMARSA) was selected as the activator. Potassium iodide (KI, Fisher Chemical), sodium hydrogen carbonate ($NaHCO_3$, Panreac), sodium thiosulfate pentahydrate ($Na_2S_2O_3{\cdot}5H_2O$, Sigma-Aldrich), and acetic acid ($C_2H_4O_2$, Sigma-Aldrich) were used for PS quantification. The DNAPL sample was obtained at Bailin landfill (Sabiñanigo, Spain) during the LIFE SURFING

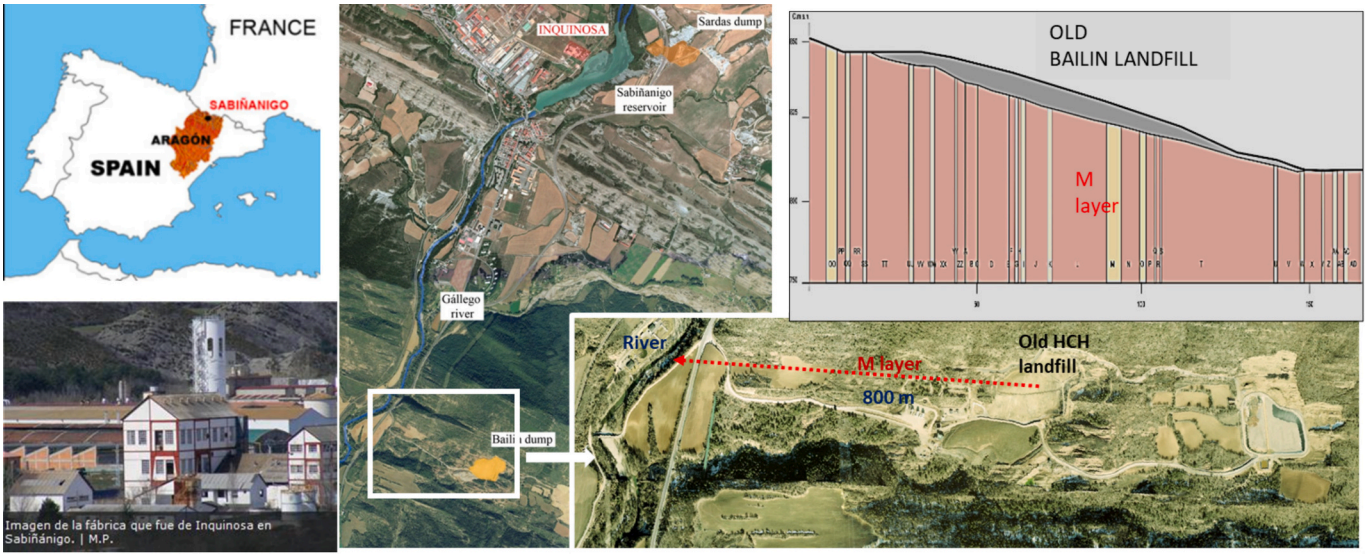


**Fig. 1.** View of Bailin Landfill and M layer.

project. This sample has been characterized, and its composition is shown in Table SM-1. In this table, the individual COCs are listed and gathered as the sum of isomers. Sodium Bromide (NaBr, provided by Panreac) was used as a conservative tracer.

### 2.2. Site description

The test cell was in the M layer beneath the old Bailin Landfill (Fig. 1). The test cell had a length of approximately 60 m, and the width of the M layer within the test cell was about 1 m along this length. There were 8 boreholes in the test cell, 6 of which were newly drilled as part of the LIFE SURFING project (see Fig. SM-3) Fractures were identified at depths up to 50 m below ground level in the test cell, although their number markedly decreased in the last 10 m. The new boreholes were executed during the LIFE SURFING project, and their testing revealed a very high level of environmental heterogeneity (see Fig. SM-4). Fractures with possible DNAPL presence were located downstream from well P194. DNAPL was detected in the fractures of newly drilled wells P195, P196, and P198. In the 1990s, installing a partial bentonite cement screen after well P172 led to the accumulation of DNAPL in wells P171 and P172, modifying the connectivity between these wells. The presence of DNAPL in wells P171 and P172 has been confirmed since 2004.

The length of the M layer from the test cell to the Gállego river was approximately 900 m, and the M layer widened from 1 m in the test cell to 3 m in the discharge zone to the river. Hydrogeological tests also determined a test cell approximate effective porosity of 0.004.

Table SM-2 lists hydraulically well-connected wells in each zone in the M layer. The table includes information on the depth of each well, its distance to well P198, ground level, and water table levels at the beginning of LIFE SURFING and before the SEAR and S-ISCO events. The last column also specifies the most common depth for groundwater sampling in SEAR and S-ISCO events.

M layer was divided into four sections (see Fig. 2).

- Test Cell (TC): Fluid injection-extraction (surfactants and oxidants) is conducted between wells P180 and P171 (60 m).
- The zone between the test cell and the barrier zone (TC-BZ, wells P171 to P127): This zone monitors the injected fluids escaping from the test cell, and alkali (NaOH) is injected to facilitate the dehydrochlorination of more chlorinated and non-aromatic COCs (see Fig. 2). DNAPL was found at the bottom of well P55 as a residual organic phase. Therefore, it is crucial to control the surfactant reaching this well beneath the test cell (299 m).
- Barrier zone (BZ), between P127 and P98 (240.1 m): This zone monitors arriving fluids, and alkali (NaOH) and oxidant (sodium persulfate) are added to some wells to break any emulsion that may have reached this zone and oxidize contaminants. In two boreholes in this barrier zone (I1 and O1), hot air is injected to volatilize chlorobenzenes, and the injected air with volatilized chlorobenzenes is extracted, passing the contaminated stream through a granular activated carbon bed.
- Monitoring zone (MZ), between well P98 and the Gállego River, P126 (348.9 m). This zone monitors arriving fluids, with actions taken in the barrier zone if necessary

Before conducting SEAR and S-ISCO tests, hydrogeological tests and 7 tracer tests (measuring conductivity and bromide) were carried out from 2020 to 2021 to determine the connectivity between the boreholes and the arrival of injected tracers from the test cell to various downstream wells (Fernández et al., 2023). These tests were conducted under injection-extraction flow conditions like those used in SEAR and S-ISCO but with tracer injection (sodium bromide and sodium chloride).

As shown in Table SM-2, the water table in the test cell was found at 15 to 27 m b.g.l. The water level values previous to the LIFE SURFING project and before the SEAR-1 and S-ISCO events are depicted in Fig. 3. A high slope (higher than 60 m) exists between the table water in the test

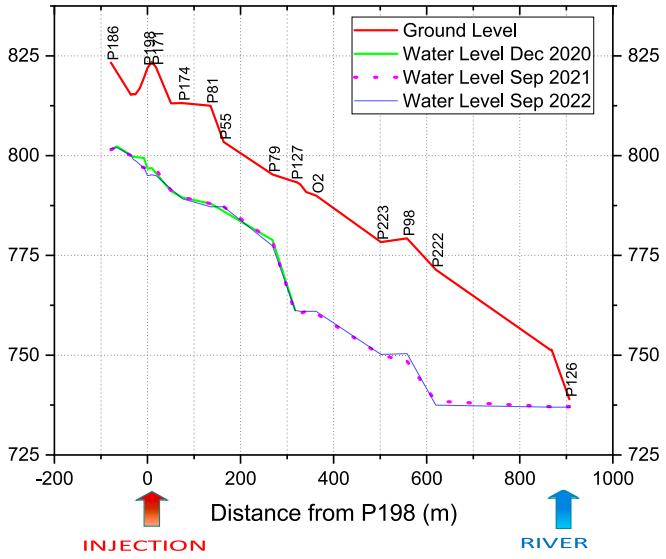


**Fig. 3.** Ground surface and groundwater levels in the M layer (from the test cell to the river, in meters) before the SEARs and S-ISCO events.

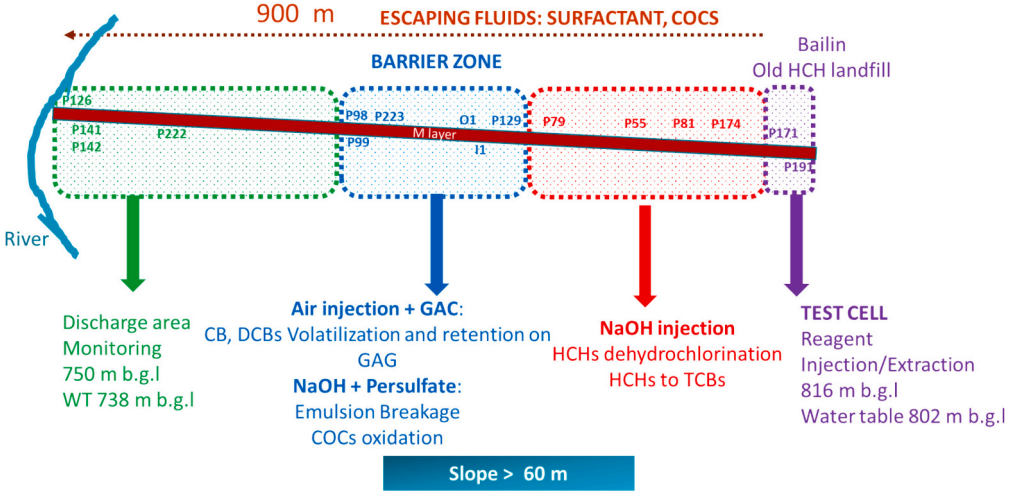


**Fig. 2.** Zones in M-Layer in LIFE SURFING.

cell and the Gallego river.

### 2.3. Procedure

#### 2.3.1. Two SEAR trials were carried out during the LIFE SURFING project. The first was held in May 2022, and the second in June 2022

The objectives of these SEAR (Surfactant Enhanced Aquifer Remediation) trials were to remove a significant portion of residual DNAPL (Dense Non-Aqueous Phase Liquid) located in the most contaminated areas of the test cell (wells 195–198 in SEAR-1 and wells 171–172 in SEAR-2). In both instances, strategies for injecting the surfactant solution with simultaneous extraction at wells downstream from the injection wells and recirculation at the injection wells were tested to ensure sufficient contact time for the solubilization of the contaminant trapped in the fractures while preventing the contaminated emulsion from escaping downstream to the river. After the injection-recirculation stage, there is a process for extracting the injected fluids and on-site treatment of the extracted contaminated emulsions. Two weeks after the last SEAR trial, vacuum extraction is performed to purge the wells where the surfactant was injected to mobilize the residual DNAPL, whose interfacial tension has been reduced by surfactant absorption, making it more easily extractable.

SEAR1:

This first SEAR test aims to solubilize the dense residual phase between boreholes P192 and P198 and recover the maximum volume of surfactant and contaminants. Before the test execution, groundwater sampling and vertical conductivity profiles were measured (baseline).

Schemes of operation in the SEAR 1 event in the test cell and the whole M layer are shown in Fig. 4 and Fig. SM-5, respectively.

As shown in Fig. 4, the surfactant solution (19.8 g/L of Emulse®, 2.5 g/L of NaCl, 190 mg/L of NaBr and 1 % $H_2O_2$) was injected in boreholes P198 and P195 (flowrates and times shown in table SM-3) during 7.6 h (460 min). The desired groundwater level (about 810 m) was reached during the injection period (initial value of the groundwater level about 800 m) with a total volume injected of 9.3 $m^3$. Pneumatic pumps were placed at P171 and P172 wells to minimize downstream losses. During the surfactant injection, the flows extracted in P171 and P172 are first recirculated (100 min) to the P195 and P198 wells, respectively. After this time, fluids extracted at P171 and P172 were sent to the decanter. After the injection of surfactant aqueous solution stops, wells P196 and P195 are equipped with electric pumps to recover the injected fluids. Extraction also continues in P171 and P172. A summary of flow rates and times for injection, recirculation, and extraction is shown in Table SM-3. A total volume of 7.1 $m^3$ of polluted groundwater with surfactants and COCs was recovered by extraction. These polluted emulsions are pumped, discharged to a decanter, and managed on-site.

As shown in Fig. SM-5, NaOH dispensers are installed in the P81, P55 and P129 wells to degrade the surfactant and the COCs leakages downstream (about 700 kg of NaOH were injected). In boreholes I1 and O1, the oxidant solution (80 g/L of sodium persulfate and NaOH at pH 12), antifoam and air were injected, and generated vapours were captured in a granular activated carbon bed. Downstream, oxidant and NaOH were also added to the P99 well. About 10 $m^3$ of the aqueous oxidant solution was injected into the barrier zone.

In addition to continuous measurements with divers, manual vertical conductivity profiles and groundwater sampling at discrete depths were carried out in 28 boreholes (Table SM-2). The pH value, conductivity, bromide, surfactant, and COC concentrations were determined in groundwater samples. The monitoring was maintained in each borehole until initial groundwater levels were recovered (or for at least 400 h).

SEAR 2:

A scheme of the operation in the SEAR 2 event in the test cell and the whole M layer is shown in Fig. 5 and Fig. SM-6, respectively.

The second SEAR test aims to solubilize the dense residual phase in wells P171 and P172 and recover the maximum volume of surfactant and contaminants. The distance between both wells is 9 m, so a push-and-pull type test was considered. As shown in Fig. 5, the aqueous surfactant solution (17 g/L of Emulse®, 3.8 g/L of NaCl, 186 mg/L of NaBr and 1 % of $H_2O_2$) is injected in wells P171 and P172 during 340 min (5.66 h). In total, 6 $m^3$ were injected. An electric pump was installed at P174, 57 m downstream of P171, to reduce the downstream leakage flow. The extracted fluid at P174 was recirculated to P198 during the first 130 min. From 130 to 500 min, groundwater was extracted in P174 with an electric pump and sent to the decanter. To recover injected fluids after the injection had finished, well P171 was equipped with an electric pump, and well P172 was equipped with a pneumatic pump. The extraction pumping is maintained in these wells from 340 to 500 min. About 6 $m^3$ of fluid was extracted in SEAR 2. Table SM-5 summarizes flow rates and injection-recirculation-extraction times in the SEAR 2 event.

The equipment of the barrier zone is maintained to degrade the surfactant and COC leakage downstream, similar to that described in the SEAR 1 event. As shown in Fig. SM-6, NaOH dispensers are installed in the P81, P55 and P129 wells to degrade the surfactant and the COCs leakages downstream (about 650 kg of NaOH were injected). In this event, 9 $m^3$ of an aqueous solution containing 80 g/L of sodium persulfate and NaOH at pH 12 was injected into the barrier zone. The oxidant injection began 2 h after the surfactant injection started and was

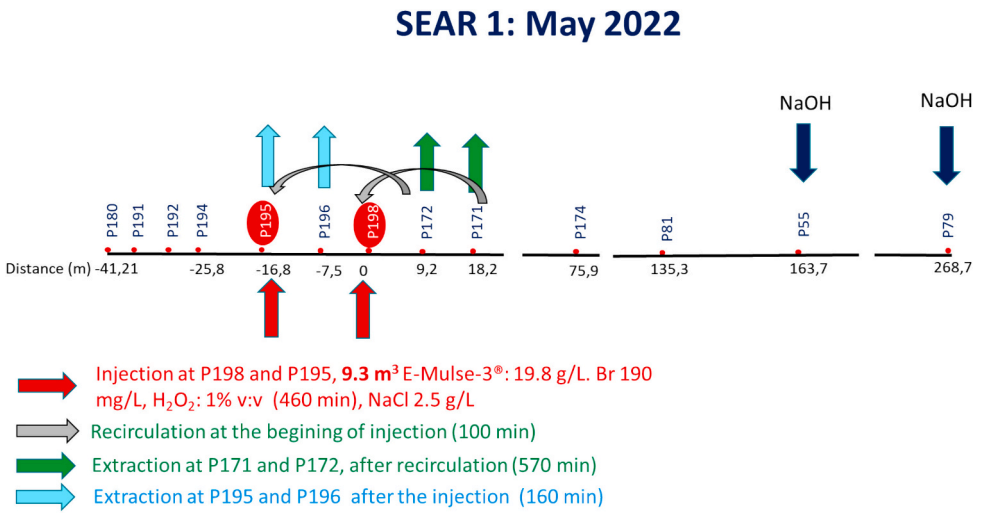


**Fig. 4.** Scheme of Operation at SEAR-1 in the test cell.

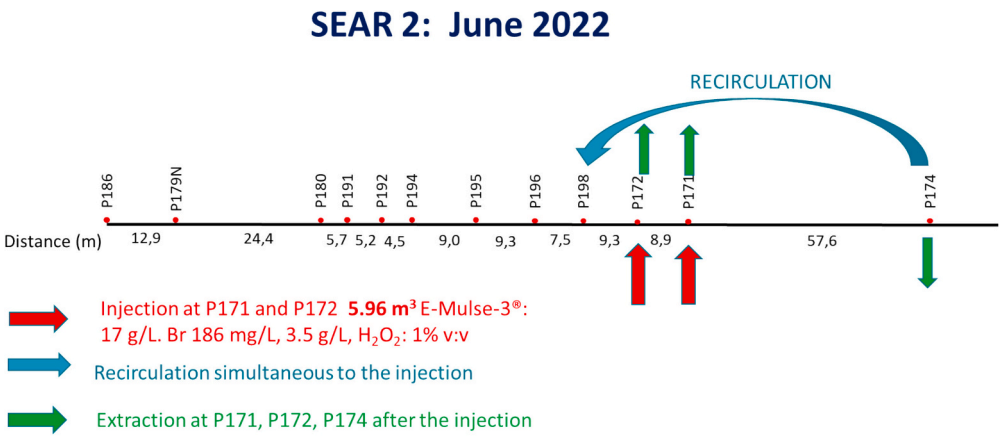


**Fig. 5.** Scheme of operation at SEAR-2 in the test cell.

maintained for 55 h in I1 and O1.

While persulfate was injected, aeration was carried out from the bottom of the same boreholes I1 and O1 and maintained for 10 days. In addition to continuous measurements with divers, manual vertical conductivity profiles and sampling at discrete depths were carried out in 28 boreholes. pH, conductivity, bromide, surfactant and COCs concentrations were determined in the groundwater samples at different times (zero time corresponds to the beginning of the surfactant injection). The monitoring was maintained in each borehole until initial groundwater levels or at least for 400 h.

Two weeks after the injection in SEAR 2, with the groundwater table stabilized, the depth of the boreholes was manually measured, and an accumulation of fines of up to 10 m was observed in those wells located in the test cell and downstream to P55. The accumulated fines were extracted with a self-priming tanker truck from wells P194 to P55.

### 2.3.2. S-ISCO

The objective of the S-ISCO trial is to eliminate the residual contamination remaining in the test cell after the application of SEAR, through the simultaneous addition of oxidants and surfactants without extraction. It is crucial to ensure sufficient contact time between the oxidant-surfactant mix and the contaminants to achieve the solubilization of the contaminants, their oxidation in the aqueous phase, and a proper balance between the competitive oxidation of surfactants and contaminants. This aims to reduce the unproductive consumption of oxidants while preventing the contamination mobilized during injection from reaching the Gallego river. The concentrations of oxidant, surfactant, and alkali are selected based on previous laboratory studies (Garcia-Cervilla et al., 2022a; García-Cervilla et al., 2021).

Twenty-two cubic meters (22 $m^3$) of the surfactant-oxidant solution, consisting of 40 g/L of $Na_2S_2O_8$, 8.75 g/L of NaOH, and 4 g/L of *E*-Mulse 3®, were injected into wells P195 and P198 in 16 pulses over 30 h in October 2022. The fluids are injected at the wellhead in P198 and P195. The average volume injected at each pulse was 1.2 $m^3$/h, with a final pulse at 44 h injecting 2 $m^3$. The sequence of injected fluids and corresponding times is summarized in Table SM-5.

To minimize groundwater entry into the test cell, thereby avoiding reagent dilution, 1 $m^3$ of the prepared oxidant-surfactant solution was dosed at a rate of 100 L/h upstream of the test cell (P179N) after the last injection of each day. An electric pump was installed in well P172 (9.3 m downstream of P198) to recirculate flows escaping downstream to the test cell back to P196.

In well P171, located 18 m downstream of P198, a solution of 5 g/L of Emulse® and 2 % Xanthan Gum was dosed at an average flow rate of 20 L/h throughout the entire SISCO injection, accompanied by simultaneous injection of airflow to generate foams.

A solution of 25 % NaOH was dosed in wells P174, P55, P79, and P98 from the beginning of the injection until 48 h after its completion to maintain the groundwater pH around 12. About 1000 kg of NaOH were injected in the S-ISCO event. In the barrier zone, aeration (5 $m^3$/h per well) and vapor extraction (6 $m^3$/h per well) were sustained in wells I1 and O1 for 14 days after injection. Foam generation in these wells was controlled by adding a siliconized defoamer.

Test monitoring was carried out with 23 fixed-level probes, with vertical conductivity profiles and groundwater sampling in 28 wells to capture the passage of the escaped fluids plume. These groundwater samples were analyzed for pH, conductivity, surfactant, persulfate, free chlorine, and COCs concentration. NaOH solution was injected 20 days after the injection in wells P171, P172, P198, and P195 to recover the alkaline pH in these wells.

A scheme of the operation in the S-ISCO event in the test cell and the whole M layer is shown in Fig. 6 and Fig. SM-7, respectively.

### 2.3.3. Monitoring post-S-ISCO

Groundwater monitoring after S-ISCO was conducted periodically (six months and one year after S-ISCO) in the M-layer wells.

## 2.4. Analysis

The aqueous phase with or without surfactant was diluted at 1:10 in MeOH or extracted with 1:4 n-hexane (volume ratios), respectively. COCs in MeOH or hexane were quantified by Gas chromatography coupled with a Flame Ionization Detector and an Electron Capture Detector (GC-FID/ECD). The chromatographic method is described elsewhere (Conte et al., 2022; Garcia-Cervilla et al., 2022b). The aqueous samples were analyzed simultaneously in the laboratories of UCM and the Government of Aragon (Pirenaium), with a difference of <12 % in the measurements.

PS in aqueous phases was measured by Iodometric titration with sodium thiosulfate. A potentiometric titration analyzer (Metrohm, Tiamo 2.3) was used. A Basic 20-CRISON pH electrode measured pH.

The concentration of the conservative tracer (bromide anion) was determined using ionic chromatography (Metrohm 761 Compact IC) with anionic chemical suppression and a conductivity detector. Details are shown elsewhere (Guadaño et al., 2022).

The conductivity of the samples was also measured in the field with a portable pH/conductivity unit (Model 914 pH/Conductometer, Metrohm). The conductivity profiles in the alluvial were also determined during event 6 using a multiparameter electrode placed at the end of a tape measure.

When the oxidant was absent, the surfactant concentration in the groundwater sample was determined using the limonene concentration (co-solvent in the commercial Surfactant *E*-Mulse 3®). The limonene mass percentage in E-Mulse 3® was approximately 15 %, as determined

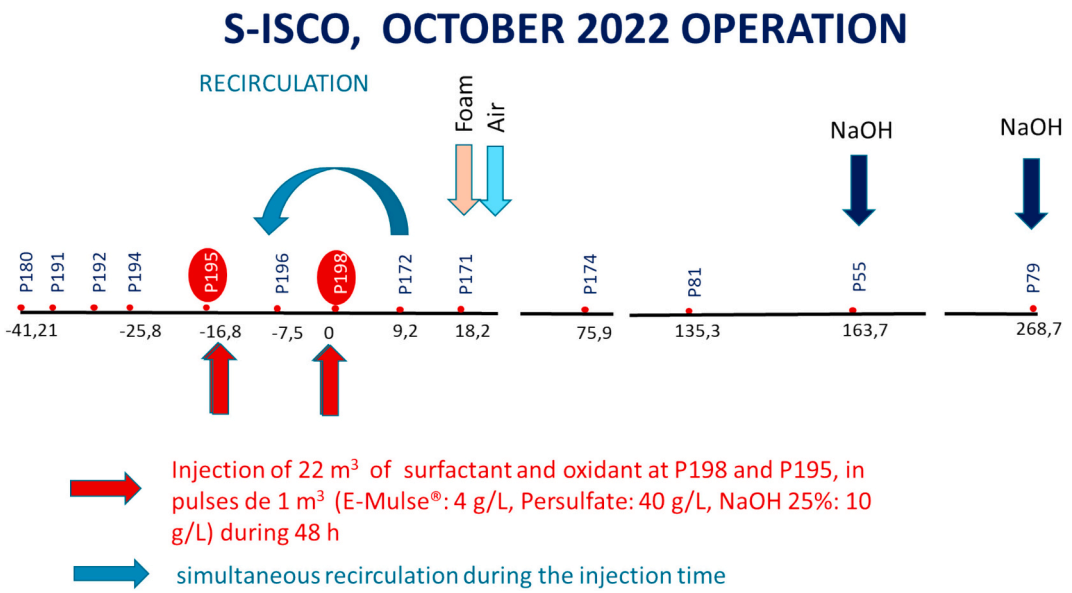


**Fig. 6.** Scheme of Operation at S-ISCO in the test cell.

by GC/FID. In the presence of an oxidant, the Equivalent Surface Capacity was measured by dilution until the Critical Micelle Concentration (CMC) of the Surfactant was reached (80 mg/L) (García-Cervilla et al., 2020) following the procedure described elsewhere (Dominguez et al., 2019).

The fluctuations in the water table level in the wells during the test were determined by measuring with a manual conductivity probe and, in some boreholes, using a level diver.

## 3. Results

### 3.1. Information from hydrogeological and tracer tests

The hydrogeological and tracer tests carried out during 2020 and 2021 confirmed that natural flow in the absence of injection can be considered negligible compared to the flow generated by injected fluids escaping from the test cell. Hydrogeological tests in the test cell revealed that fluid injection increased the water level by several meters in the unsaturated zone (depending on the injection rate). This increase allowed the surfactant and oxidant to reach this zone, where residual DNAPL could accumulate in fractures.

The maximum injection rate was selected at around 20 L/min to reach a maximum water table level of about 10 m (reaching 810 m in the test cell), preventing the injected fluid from reaching the layers adjacent to the M layer through the top of the unsaturated zone. The communication between adjacent sandstone and limestone layers was significant in the upper 10 m from the ground level. Upon ceasing injection, water table levels recovered in <24 h in the test cell.

Tracer tests involving injection and fluid extraction in the test cell (simulating SEAR tests) recovered 50–70 % of the injected tracer.

It was observed that fluids escaping downward from the injection point in the test cell caused a rise in the water table level of the well. Water table levels before injection were restored in wells P174 to P79 <48 h after the tracer reached those wells. From wells P174 to P79, it was found that the increase in piezometric level could be related to the instantaneous flow passing through the well using the Eq. (1).

$$Q_{well}\left(\frac{m^3}{h}\right) = \Delta h(m)^{*}0.061\ m^2\ h^{-1}\ (from\ well\ P174 - P79) \quad (1)$$

where $Q_{well}$ represents the instantaneous flow rate in the well, and $\Delta h$ represents the corresponding increase in the piezometric level of the well relative to the water level before the tracer injection.

On the contrary, the injected fluid reaching the barrier zone (wells P127 to P98) raised the water table in this area, but the subsequent decline was much slower (no decreases in water levels were observed in this zone for up to 400 h). Tracer tests revealed that the injected fluid in the test cell escaping downstream was retained in the barrier zone for >400 h.

In the barrier zone, the water table rose with the arrival of injected fluids in the test cell, and there was a prolonged subsequent decrease, ensuring an extended contact time for fluids escaping from the cell in this barrier zone. This slight decrease in the attained water level resulted in diluting injected fluids downstream of the barrier zone and almost negligible tracer concentration reaching the river. This behaviour minimized the risk of surfactants and solubilized contaminants escaping from the test cell and reaching the Gállego River. The accumulation of fluids escaping from the test cell in the barrier zone ensured sufficient reaction time between the surfactants and solubilized contaminants reaching this zone and the oxidants added in the barrier zone or the remaining concentrations of oxidants arriving with the injected fluids in the test cell. The barrier zone behaved like a discontinuous reactor with a reaction time of over 400 h.

### 3.2. SEAR events

SEAR 1

The summary of injected and extracted fluids over time is presented in Table SM-3. Table SM-6 details the concentrations of COCs and surfactants in wells P171, P172, P195, and P196 before, during, and after the extraction period. Initial COC concentrations in the wells correspond to the baseline at time = 0. It is important to note that the concentration of chlorobenzene was occasionally underestimated, particularly at zero time, due to volatilization during sampling and transport.

In Table SM-6, the sum of non-aromatic compounds (NACs), Eq. (2), has also been provided.

$$NACs = PentaCXs + HCHs + HexaCXs + HeptaCHs \quad (2)$$

Table SM-6 also includes information on surfactant (through limonene) and bromide concentrations. The extraction period is highlighted in blue. Observations indicate that the surfactant injected reached wells P171 and P172 during the injection period, approaching the injected surfactant concentration values (19.8 g/L). During injection, bromide concentrations in wells P171 and P172 approached the injected values

(147 mg/L of $Br^-$).

Surfactant concentrations found in wells P195 and P196 during fluid extraction after the surfactant injection ceased were lower than those observed in the fluid extracted from wells P171 and P172 during injection. This difference may be attributed to the dilution and adsorption of surfactants during extraction after the injection. Notably, variations at 8.28 h between bromide concentrations in wells P195 and P156 (139 mg/L in P195–149 mg/L in P196), about injected values (147 mg/L), and E3 concentrations in these wells (8.81 g/L in P195 and 9.92 g/L in P192), about injected values, (19.8 g/L) confirm surfactant adsorption over time.

The concentration of COCs in the extracted fluids significantly increases with the rise in surfactant concentration in groundwater. The highest concentration of solubilized COCs occurred in well P172 at 4.28 h (3267 mg/L) with a surfactant concentration of 17.8 g/L. The Mass Solubility Ratio (MSR) of E3 with this DNAPL under equilibrium conditions between organic and aqueous phases was previously determined elsewhere (García-Cervilla et al., 2020), indicating a linear MSR value of approximately 1 g of DNAPL solubilized with 1 g of E3 (up to 10 g/L of surfactant).

The absence of a higher concentration of COCs in the emulsion despite the elevated surfactant concentration can be partly explained by the fact that equilibrium has not been achieved with DNAPL remaining as residue in the fractures. In studies conducted at the laboratory scale, the time required to reach equilibrium conditions between the organic and aqueous phases was <6 h at surfactant concentrations higher than 15 g/L (García-Cervilla et al., 2020). However, it is anticipated that the contact time required would be longer in fractured media due to the obstructive effect of the fractures. Considering the balance between increasing the contact time and preventing the escape of part of the injected fluid downwards and surfactant adsorption, injection times of about 6 h were chosen. Additionally, the extracted fluid is a mixture of aqueous phases in contact with areas of varying DNAPL concentration, causing dilution of the solubilized COCs in the most polluted areas.

The distribution of COCs in the emulsion is compared in Fig. 7 with that of COCs in the organic phase (DNAPL) obtained from well P172 before the LIFE SURFING project.

The COC distribution obtained in the sample from well P196 at time zero is also presented in the same fig. A notable similarity is observed between the distribution of COCs in the emulsion and the organic phase, confirming that the surfactant used dissolves the COCs composing the DNAPL non-selectively.

The solubilization of COCs without surfactant favours compounds with lower chlorine content, such as chlorobenzene and dichlorobenzene. The use of surfactant, therefore, enables more effective extraction of highly chlorinated compounds compared to the traditional pump and treat technique.

The concentration of COCs was measured in the extracted volume in SEAR 1 (7.1 $m^3$). An average value of 421 mg COCs/L was obtained, with a distribution like that in the emulsion samples shown in Fig. 1. The total mass of COCs extracted was about 3 kg. The mass of bromide recovered (0.83 kg $Br^-$) in the extracted fluid was approximately 60 % of the injected bromide (1.33 kg $Br^-$) and the mass of E3 recovered (54 kg) was only 30 % of the injected surfactant (180.2 kg). This disparity in surfactant recovery compared to the recovery of the conservative tracer implies the adsorption of the surfactant in the fractures or its absorption in the DNAPL within the fractures. Considering a porosity of 0.004, an average height of 0.002 m for each fracture, and the distance between the injection and extraction wells (approximately 31 m), surfactant adsorption ranged from 30 to 60 mg of E3/$m^2$ of fractures. This finding aligns with measurements conducted at the laboratory scale using cores recovered from newly drilled wells P198 and P195.

During the injection and extraction stages, the water table levels in the test cell rise (about 10 m) and fall, respectively. Within 48 h, they return to their initial values in the test cell. Unrecovered bromide may have remained in the test cell or exited with the injected fluids escaping downward. Among the wells located between P174 and P79, water levels are observed to rise and subsequently fall, recovering to initial values. The mass flow of bromide over time passing these wells is obtained by applying Eq. (3).

$$F_{Br}^{-}\left(\frac{g}{h}\right) = Q\left(\frac{m^3}{h}\right) C_{Br}^{-}\left(\frac{g}{m^3}\right) \tag{3}$$

Instantaneous flow rate $Q$ is obtained using Eq. (1). $C_{Br}^{-}$ is the measured bromide concentration in the wells between P174 and P79 at each time. Fig. SM-8 displays the bromide results passing through well P79. The mass of bromide that has passed through the well downwards the injection point is obtained as the integral given in Eq. (4)

$$m_{Br^-} = \int_{t_i}^{t_f} F_{Br}^{-}\left(\frac{g}{h}\right) dt \tag{4}$$

being $t_i$ and $t_f$ the time corresponding to the water table begins to rise in the well and the baseline is recovered in that well, respectively.

For well P79, it is determined (Fig. SM-8) that the mass of bromide passing through the well is 542 g, corresponding to 40 % of the injected bromide. This result aligns with the bromide recovered in the extracted volume in SEAR 1. Approximately 40 % of the injected fluid in SEAR 1 escaped from the test cell.

In Fig. 8, the profiles of total COCs (a), NACs (b), TCBs (c), TetraCBs (d), Emulse (e), and pH (f) are shown with distance from P198 (x-axe) and time since injection (y-axe). Distances from each well to well P198 are indicated in Table SM-2. It is observed that:

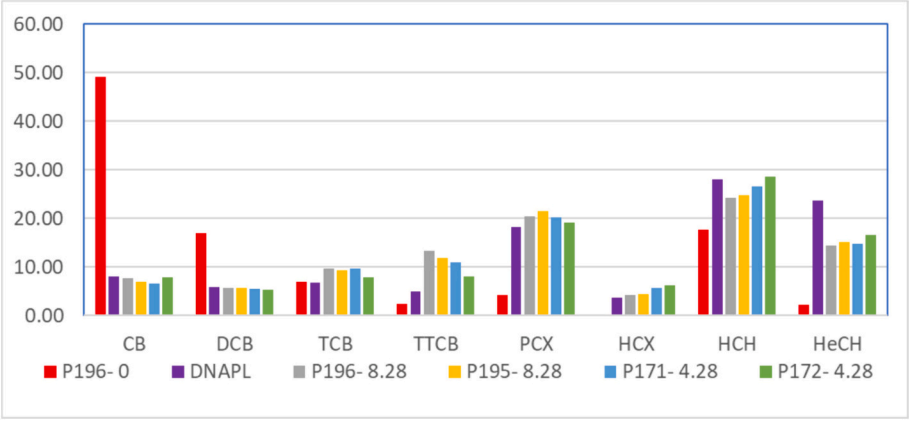


**Fig. 7.** COCs distribution in DNAPL in P171 and emulsion extracted in SEAR 1. The well and the time elapsed since the injection begins are also indicated. P196–0 corresponds to the COCs distribution solubilized in groundwater without surfactant.

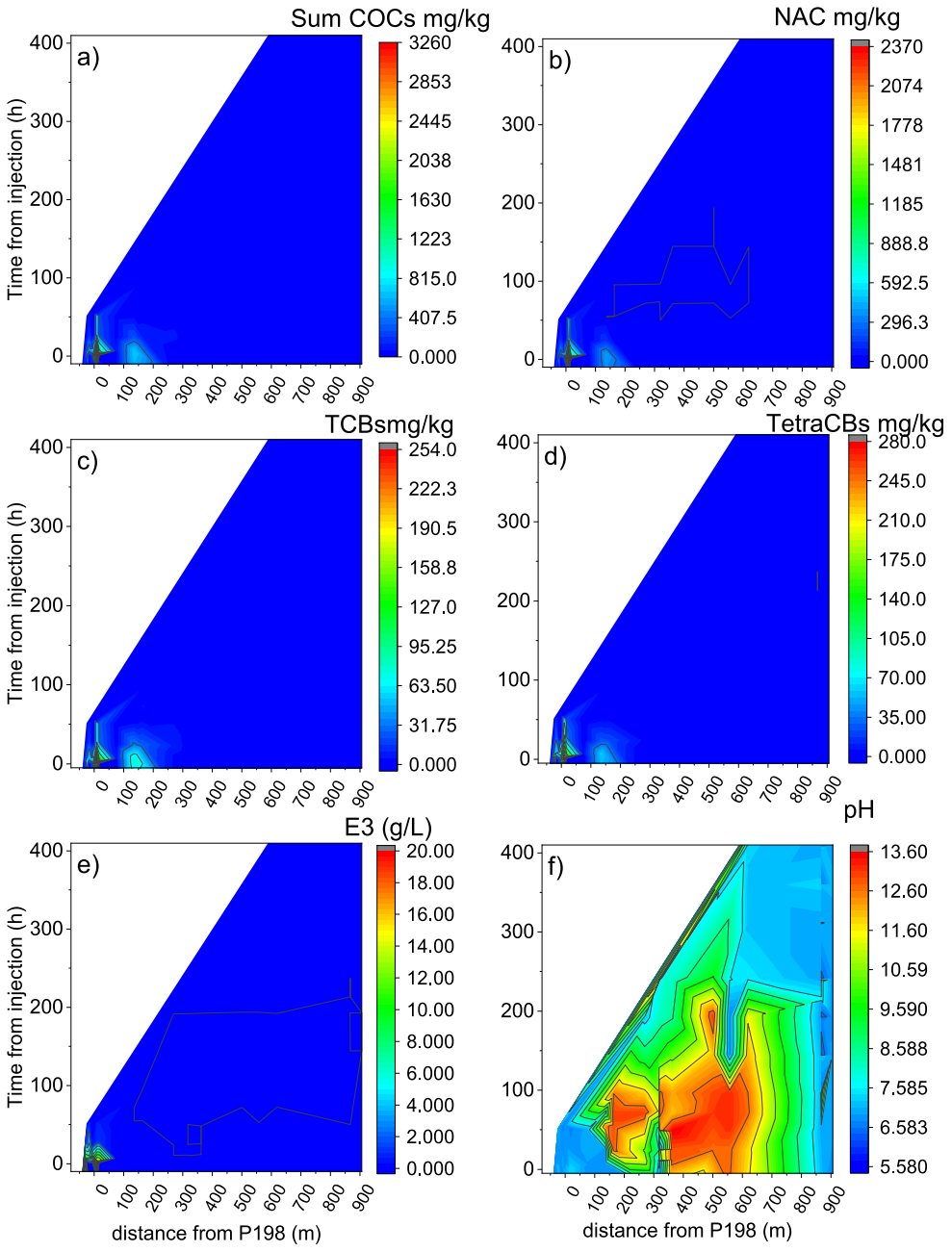


**Fig. 8.** Results obtained in SEAR 1- event. a) sum of COCs b) NACs, c) TCBs, d) TetraCBs, e) Emulse-3®, and f) pH.

- The concentration of COCs increases significantly in the test cell during the injection and extraction time (Fig. 8a) in the SEAR event. This increase is associated with the presence of surfactant (Fig. 8e). The surfactant concentration decreases in the test cell due to adsorption, which reduces solubilized COCs.
- Surfactant adsorption (Garcia-Cervilla et al., 2021) explains its confinement in the test cell and minimal detection in downstream wells. This adsorption also limits the arrival of high concentrations of solubilized COCs downstream (Fig. 8a, b, c, d).
- The concentration of COCs decreases as it advances through the M layer, although there is a rebound at P55 (166 m from P198) due to residual DNAPL at the bottom of this well (Fig. 8a, b, c, d).
- Alkali injection in wells P55 and P79 and the oxidant-alkali mixture in wells I1, O1, and 99 led to significant alkalization in the area before and the barrier zone (Fig. 8f). Associated with this alkalization is a decrease in NACs (b) in favour of an increase in TCBs (Fig. 8c) and tetraCBs (Fig. 8d) due to dehydrochlorination reactions (Fig. SM-2).
- The concentration of COCs reaching the barrier zone is very low due to surfactant adsorption along the M layer, reducing solubilized COCs. Actions in the barrier zone ensure that the concentration of COCs reaching wells near the river does not increase compared to values before the SEAR 1 trial.

SEAR 2.

The summary of injected and extracted fluids over time is presented in Table SM-4. Table SM-7 details the concentrations of COCs and surfactants in extraction wells P171, P172, and P174 before, during, and after the extraction period. The initial COC concentrations in the wells correspond to the baseline at time = 0.

Table SM-7 also includes information on surfactant (via limonene analysis) and bromide concentrations. The extraction period is

highlighted in blue. Observations indicate that the surfactant injected into wells P171 and P172 (17 g/L) reaches the well P174 during the injection period. However, the surfactant concentration decreases from P172 to P174 (Table SM-7 and Fig. SM-9) due to surfactant adsorption. Smaller differences are observed between the injected bromide (144 mg/L) and the bromide reaching P174 during the injection period (Table SM-7 and Fig. SM-9). After the injection is finished, both surfactant and bromide concentrations in wells P171, P172, and P174 decrease with extraction. The decrease in well P172 is less pronounced than in the other two wells due to the lower flow rate used in this well (Table SM-4).

The high surfactant concentration reaching wells P171, P172, and P174 results in a significant solubilization of COCs. During fluid extraction, COCs concentrations in wells P171 and P172 reach values of up to 2500 mg/kg, while the COCs concentration in P174 during fluid extraction is notably higher (up to 5000 mg/kg), confirming the presence of a significant residual DNAPL between wells P172 and P174. COCs distribution in the solubilized DNAPL was like that shown in Fig. 7. Approximately 7 kg of COCs were extracted in the SEAR 2 event as solubilized COCs in the 6 $m^3$ extracted fluid (with an average concentration in the extracted fluid of 1183 mg/L).

In Fig. 9, the profiles of total COCs (a), NACs (b), TCBs (c), TetraCBs (d), Emulse (e), and pH (f) are shown with distance from P198 (x-axe) and time since injection (y-axe). Distances from each well to well P198 are indicated in Table SM-2. It is observed that:

- The concentration of COCs remains elevated between wells P172 and P55 due to the concentration of surfactant in injected fluids and the presence of DNAPL (Fig. 9a).
- The concentration of solubilized COCs is prolonged in well P172 (Fig. 9 a) with time due to the low extraction flow rate used in this well (see table SM-7, SM-4).
- The concentration of COCs significantly decreases from well P55 onwards, attributed to the absence of DNAPL past this well and a

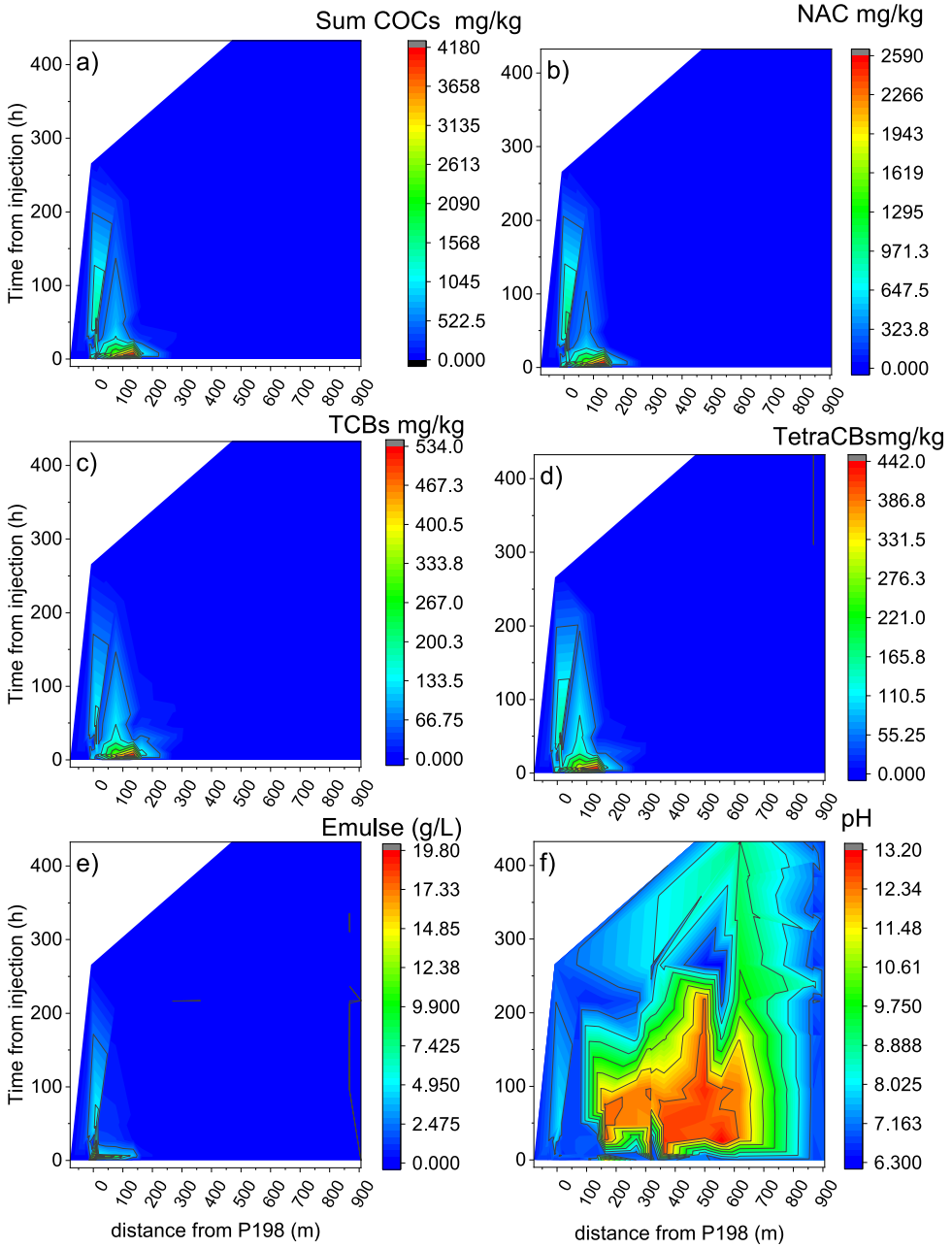


**Fig. 9.** Results obtained in SEAR 2- event. a) sum of COCs b) NACs, c) TCBs, d) TetraCBs, e) Emulse-3®, and f) pH.

notable reduction in surfactant concentration downstream of P55 (see Fig. 9 e).

- The injection of NaOH from well P81 produces a strongly alkaline pH, maintained between wells P81 (135 m from P198) to P98 (600 m from P198) for 100 to 200 h, potentially aiding in emulsion breakdown and significant disappearance of non-aromatic compounds (NACs) due to dehydrochlorination (see Fig. 9 b and Fig. 9 f).
- No increase in the concentration of COCs has been observed in the wells leading to the Gállego River throughout the entire SEAR2 trial (Fig. 9 a, b, c, d).

Two weeks after the injection in SEAR 2, with the groundwater table stabilized, the depth of the boreholes was manually measured. An accumulation of fines of up to 10 m was observed in the wells in the test cell (P171, P172, and P174) and downstream (P55). The accumulated fines were extracted with a self-priming tanker truck. 12 $m^3$ of leachate and fines were extracted, containing approximately 10 kg of DNAPL in solution and 90 kg of DNAPL mixed with the fines. The total DNAPL extracted in the SEAR events was about 110 kg. The mass of surfactant added in these trials was approximately 290 kg. The mass ratio of added surfactant to recovered DNAPL is approximately 2.6 kg per kg of DNAPL. This value is considered sufficiently low, especially considering the low DNAPL recovery by pumping since 2016 (see Fig. SM-1) and the medium complexity (fractured sandstones).

### 3.3. S-ISCO

The summary of injected fluids in P198 and P195 over time is presented in Table SM-5. Table SM-8 provides details on the COCs, oxidant and surfactant concentrations and pHs in wells of the test cell (P171, P172, P198, P195, P194, and P192), during (0–45 h), and after the injection of oxidants and surfactants (up to 467 h). The initial COC concentrations in the wells correspond to the baseline at time = 0. Chlorobenzene concentrations have been underestimated in some samples due to volatilization during sample transportation and measurement.

In Fig. 10, profiles of total chlorinated organic compounds (COCs) (a), NACs (b), sum of TCBs+TetracBs (c), persulfate (PS) (d), surfactant

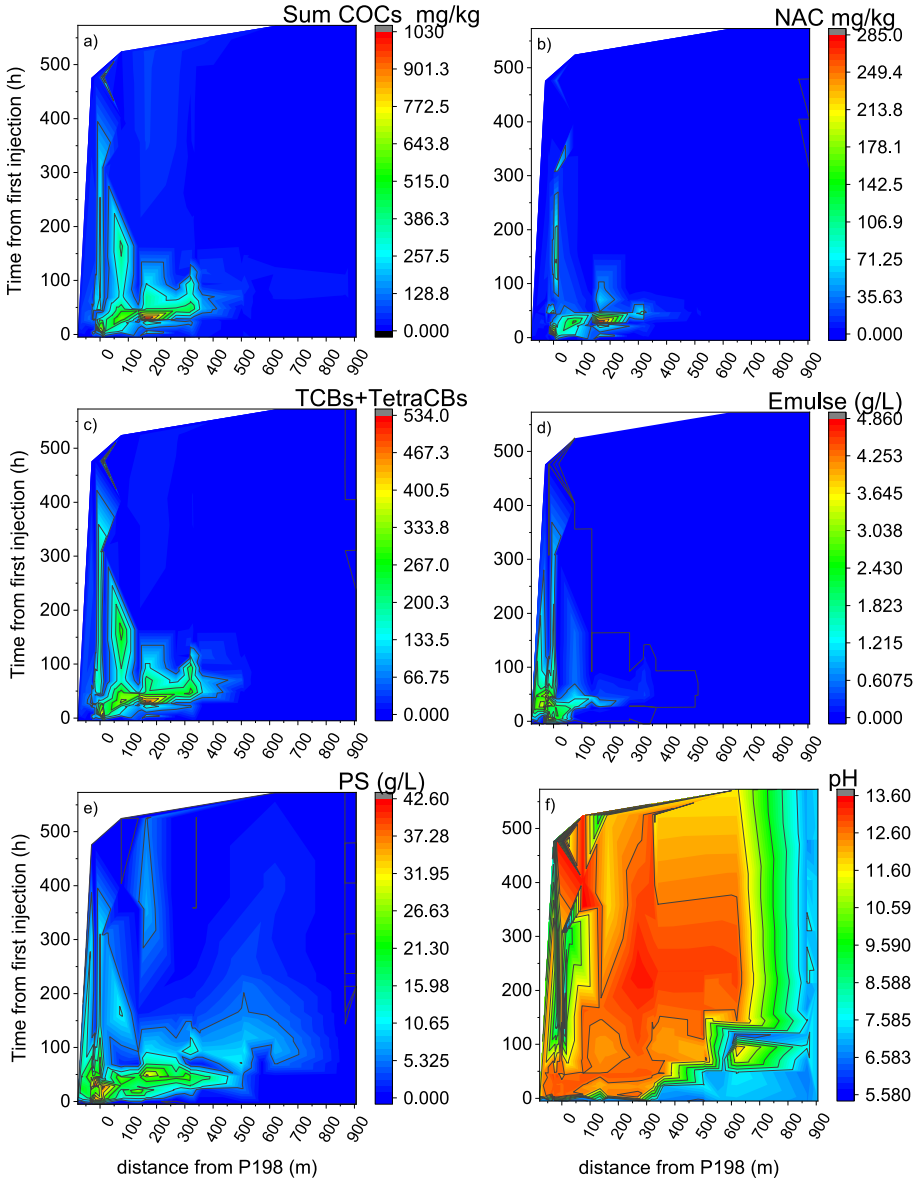


**Fig. 10.** . Results obtained in S-ISCO- event. a) Sum of chlorinated organic compounds (COCs, b) NACs c) sum of TCBs+TetracBs d) persulfate (PS) e), surfactant and f) pH.

(e), and pH (f) are displayed as a function of distance from P198 (x-axis) and elapsed time since injection (y-axis). Distances from each well to well P198 are indicated in Table SM-2.

The evolution of water table levels in the wells, from the test cell to the river, is depicted in Figs. SM-16, SM-17, SM-18, and SM-19. In Fig. SM-10, modifications in water levels within the test cell due to injection pulses are observed. However, by the 70-hour mark, these water levels have returned to their initial values. Fluids escaping downstream from the test cell (totalling 22 $m^3$ injected) result in elevated water levels in wells P174, P81, P55, and P79, effectively restoring the initial water table values before the 200-hour threshold, except for well P79, which does not fully reach the initial value (as shown in Fig. SM-11).

In the barrier zone (Fig. SM-12), an initial increase in water levels before 100 h is noticed, attributed to the arrival of fluid escaping from the test zone. However, following this initial rise, water levels remain relatively constant throughout the extensive monitoring period of over 400 h (Fig. SM-12). As previously noted in the hydrogeological test results, this corresponds to an accumulation of injected fluid that escapes from the test cell within this barrier zone, providing additional time for oxidation reactions and emulsion breakdown. After a prolonged time (>500 h), the gradual release of accumulated fluid downstream happened, leading to a return to normal water table levels. Nevertheless, this reduction process is notably slow and dilutes the wells downstream of the barrier zone.

Consequently, the gradual release of fluids from the barrier zone over time will not result in an elevated concentration of contaminants downstream (as depicted in well P222 in Fig. SM-13). The wells near the river demonstrate a very marginal, nearly imperceptible increase in water levels during the monitoring period (as observed in well P141 in Fig. SM-13).

Fig. 10 illustrates the accumulation of chlorinated contaminants before the barrier zone (Fig. 10 a). Beyond 400 m from well P198, contaminant concentrations are low, similar to the initial values before the LIFE Surfing project. This finding confirms the extended retention time in the barrier zone for fluids that escaped from the test cell. The surfactant concentration (Fig. 10e) decreases with increasing distance from the injection point, eventually disappearing due to soil adsorption and emulsion breakdown, which is induced by the alkaline pH and the remaining oxidant.

The pH remains consistently alkaline within the test cell for a minimum of 100 h, with a subsequent alkaline shift resulting from the injection of NaOH at 400 h. This alkali injection within the area between the test cell and the barrier zone and within the barrier zone itself ensures an alkaline pH for over 400 h (Fig. 4f).

Persulfate maintains relevant concentrations in the test cell for at least 70 h and in the barrier zone for nearly 100 h (Fig. 4d), all under alkaline conditions. This duration is ample for the oxidation of contaminants that were either retained in the test cell or transported downstream from the test cell along with the fluids that escaped after the injection of oxidants and surfactants. Due to the alkaline conditions, chlorinated contaminants are primarily present as trichlorobenzene and tetrachlorobenzene (Fig. 10c), with significantly lower concentrations of non-aromatic chlorinated compounds, including hexachlorohexanes (HCHs)) (Fig. 4b). The.

In well P55, located 163 m from the injection point, there is a noticeable increase in contaminant concentration due to a dense phase in the bottom of this well (Fig. 4a, b, c). Nonetheless, these contaminants that enter the fluid descending from the test cell are also oxidized within the barrier zone.

Finally, a mass balance of contaminants passing through the wells between the test cell and the barrier zone was accomplished to estimate the mass of contaminants that escaped from the test cell and were subsequently oxidized. This calculation involved assessing the instantaneous flow through wells P174, P81, P55, and P79, situated between the test cell and the barrier zone, and where water table levels were restored before 200 h. Since water table levels in the test cell were restored before 70 h, all the injected volume within the test cell (totalling 22 $m^3$) has migrated downstream. The mass of chlorinated contaminants, $m_j(g)$, passing through each well (P174, P81, P55, and P769) at a given time, factoring in concentration and instantaneous flow rate, was determined using Eq. (5)

$$m_j(g) = \int_{t_i}^{t_f} Q_{well\,t}\left(\frac{m^3}{h}\right) C_{j_t}\left(\frac{g}{m^3}\right) dt\ (h) \tag{5}$$

Table 1 presents the mass of contaminants that passed through each well between the test cell and the barrier zone. This table also includes the mass of surfactants that passed through the wells.

The mass of contaminants retained in the test cell after injection, which has gradually oxidized over time (not calculated), must be added to the mass of contaminants shown in Table 1. Thus, while it is challenging to estimate precisely the total mass of oxidized contaminants precisely, this value can be estimated at least 20 kg. This fact implies a mass ratio of persulfate to the contaminant of approximately 44 kg: kg. The stoichiometric ratio of persulfate for alkaline activation to achieve the complete mineralization of that mass of chlorinated organic compounds (COCs), assuming an average molecular weight of 210 g/mol, would be 32 kg: kg (630 kg of PS). The injected oxidant mass was 880 kg, indicating that there was not a significantly unproductive consumption of persulfate. The surfactant mass per kilogram of oxidized chlorinated contaminants has been approximately 4.5.

The residence times between the injection zone and the barrier zone have exceeded 200 h (Fig. SM-12), with the concentrations of oxidant and alkali remaining sufficiently high during this period Fig. 10. These conditions ensure contaminant removal and are consistent with the kinetics observed in laboratory studies (Garcia-Cervilla et al., 2022a; Santos et al., 2018b).

### 3.4. Monitoring post-LIFE

The concentrations of chlorinated organic compounds in the test cell and downstream of it were monitored before, during, and after the Life Surfing trials. Representative data from this monitoring, conducted before the execution of the SEAR and S-ISCO trials (February 2021) and one year after the completion of these trials (October 2023), are presented in Fig. 5. The compounds have been grouped into Chlorobenzenes (CBs = CB + DCBs+TCBs+TetraCBs) and HCHs ($\alpha, \beta, \gamma, \delta$ *and* $\varepsilon$). The concentration of HCHs (the most chlorinated and toxic compounds) has significantly decreased both within the test cell and up to the barrier zone after the application of SEAR and S-ISCO. Furthermore, this decrease is sustained one year after the conclusion of S-ISCO in the LIFE Surfing project (Fig. 11).

Furthermore, it has been observed that the amount of DNAPL accumulated at the bottom of the piezometers in the test cell (P98, P171, and P172) has notably decreased following the SEAR and S-ISCO trials. This residual phase has not been detected in these wells at least one year after the completion of these trials, confirming the more effective elimination of residual DNAPL in the test cell compared to traditional pneumatic

**Table 1**
Mass of Contaminants and oxidants passing through the wells P174 to P79.

| Compound | P174 | P81 | P55 | P79 |
|---|---|---|---|---|
| Emulse (kg) | 21.0 | 6.6 | 10.3 | 1.6 |
| CBs (g) | 911 | 402 | 1017 | 516 |
| DCBs (g) | 1362 | 651 | 2016 | 753 |
| TCBs (g) | 2636 | 1217 | 3205 | 1026 |
| TetraCBs (g) | 2884 | 1325 | 3387 | 748 |
| PentaCX (g) | 918 | 268 | 1531 | 177 |
| HexaCX (g) | 9.1 | 1.1 | 20.5 | 0.8 |
| HCH (g) | 662 | 163 | 1054 | 74 |
| HeptaCH (g) | 7.7 | 2.0 | 26.8 | 0.8 |
| NAC (g) | 1597 | 434 | 2633 | 252 |
| Sum COCs (g) | 9475 | 4075 | 12,365 | 3322 |

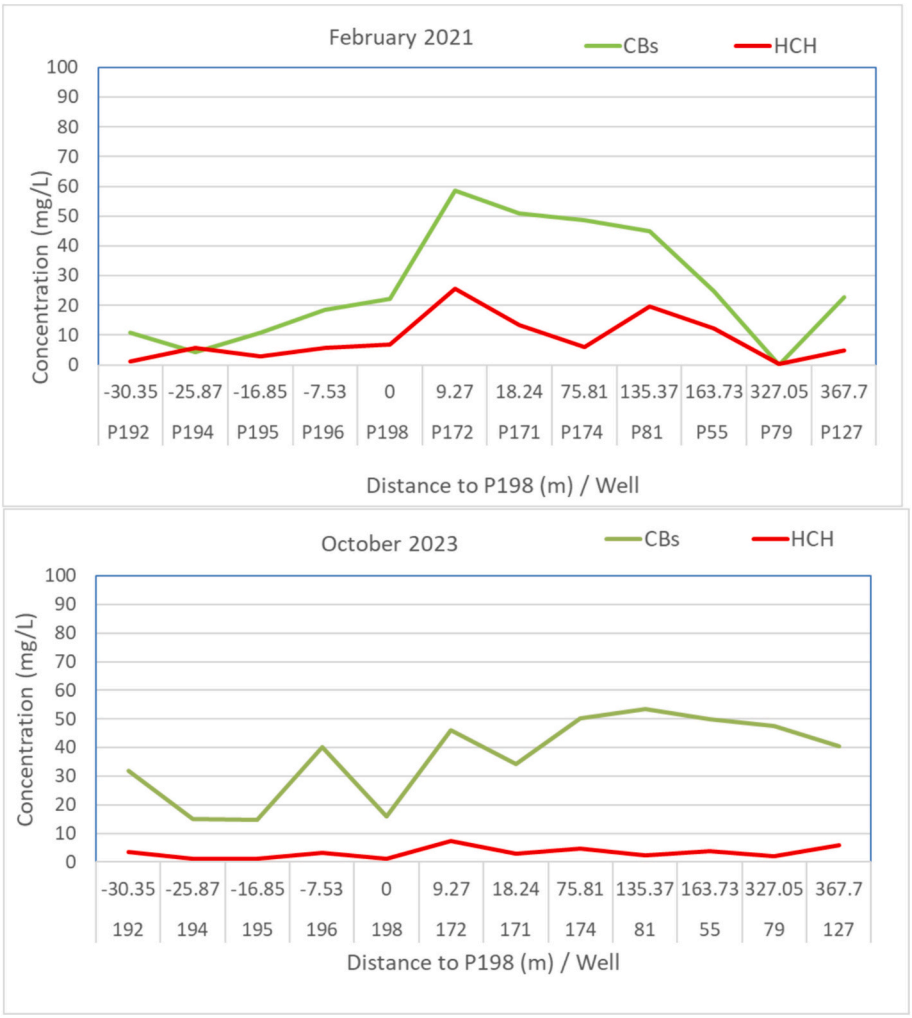


**Fig. 11.** Concentration of Chlorobenzenes (CB + DCBs+TCBs+TetraCBs) and HCHs in groundwater before (February 2021 and one year after S-ISCO in LIFE SURFING Project) in the Test Cell (P192-P171) and before the barrier zone (P174-P127).

pumping methods (Fig. SM-2).

This pilot trial should continue to be monitored, and the application of SEAR and S-ISCO treatments should be repeated over time, especially downstream, focusing on well P55 to reduce chlorinated contaminants further.

## 4. Conclusions

The LIFE SURFING project, employing Surfactant Enhanced Aquifer Remediation (SEAR) and In Situ Chemical Oxidation enhanced by Surfactant (S-ISCO) techniques, was successfully executed at the Bailin Landfill in Sabiñánigo, Spain. This site is characterized by fractured lithology, deep slopes, and proximity to a sensitive receptor (the Gállego River). There are no known precedents for applying SEAR and S-ISCO in such sites. Through the careful selection of injection (and extraction in SEAR) strategies, appropriate concentrations of reactants, and downstream control measures, significant DNAPL removal was achieved, surpassing the limitations of traditional DNAPL extraction methods. For the successful real-scale application of SEAR and S-ISCO, it is crucial to understand the kinetics and equilibria of contaminant solubilization, surfactant adsorption and absorption, and competitive oxidation between surfactants and oxidants through laboratory studies, as well as to determine the flow of injected fluid at the site using tracer tests.

The SEAR treatment effectively solubilized and mobilized Dense Non-Aqueous Phase Liquids (DNAPLs), which were found to be a residual phase in the landfill's most contaminated area, known as the Test Cell. Approximately 130 kg of DNAPL were removed during the SEAR trials. Moreover, a significant percentage of the injected tracer and surfactant was recovered, indicating efficient contaminant extraction. Contaminated emulsions were adequately managed on-site.

The application of S-ISCO, involving the injection of a solution of persulfate, surfactant, and NaOH, resulted in the oxidation of about 20 kg of DNAPL, maintaining low concentrations of toxic and chlorinated compounds one year after the project's completion.

Implementing a barrier zone between the test cell and the river, which included alkali dosing, aeration, vapor extraction, and oxidant injection, was pivotal in preventing the migration of injected contaminants to the river. The project involved extensive monitoring and detailed groundwater composition analysis, vital for assessing the effectiveness of the techniques and guiding decision-making. Hydrological and tracer tests conducted before the SEAR and S-ISCO events also yielded valuable data, contributing to the effective design and execution of the remediation strategies.

The encouraging outcomes of the LIFE SURFING project indicate that these advanced remediation techniques could be successfully applied to other sites contaminated with DNAPLs.

## CRediT authorship contribution statement

**Jesús Fernández:** Writing – review & editing, Writing – original

draft, Methodology, Investigation, Formal analysis, Conceptualization. **David Lorenzo:** Writing – review & editing, Methodology, Investigation, Formal analysis, Data curation. **Jorge Net:** Writing – review & editing, Investigation. **Elena Cano:** Writing – review & editing, Investigation. **Patricia Saez:** Investigation, Data curation. **Carlos Herranz:** Writing – review & editing, Investigation. **Carmen M. Domínguez:** Writing – review & editing, Investigation. **Salvador Cotillas:** Writing – review & editing, Investigation. **Aurora Santos:** Writing – review & editing, Writing – original draft, Supervision, Investigation, Funding acquisition, Formal analysis, Data curation, Conceptualization.

## Declaration of competing interest

The authors declare that they have no known competing financial interests or personal relationships that could have appeared to influence the work reported in this paper.

## Data availability

Data will be made available on request.

## Acknowledgements

This work was supported by the EU Life Program (LIFE17 ENV/ES/000260) and the Aragon Government.

## Appendix A. Supplementary data

Supplementary data to this article can be found online at https://doi.org/10.1016/j.scitotenv.2024.173260.

## References

Abriola, L.M., Christ, J.A., Pennell, K.D., Ramsburg, C.A., 2012. Source remediation challenges. In: Kitanidis, P.K., McCarty, P.L. (Eds.), Delivery and Mixing in the Subsurface: Processes and Design Principles for in Situ Remediation, pp. 239–276.

Akyol, N.H., 2018. Surfactant-enhanced permanganate oxidation on mass-flux reduction and mass removal (MFR-MR) relationship for pool-dominated TCE source zones in heterogeneous porous media. Water Air Soil Pollut. 229 https://doi.org/10.1007/s11270-018-3946-3.

Barbati, B., Lorini, L., Amanat, N., Bellagamba, M., Galantini, L., Papini, M.P., 2023. Enhanced solubilization of strongly adsorbed organic pollutants using synthetic and natural surfactants in soil flushing: column experiment simulation. J. Environ. Chem. Eng. 11. https://doi.org/10.1016/j.jece.2023.110758.

Besha, A.T., Bekele, D.N., Naidu, R., Chadalavada, S., 2018. Recent advances in surfactant-enhanced in-situ chemical oxidation for the remediation of non-aqueous phase liquid contaminated soils and aquifers. Environ. Technol. Innov. 9, 303–322. https://doi.org/10.1016/j.eti.2017.08.004.

Cheng, M., Zeng, G., Huang, D., Yang, C., Lai, C., Zhang, C., Liu, Y., 2017. Advantages and challenges of tween 80 surfactant-enhanced technologies for the remediation of soils contaminated with hydrophobic organic compounds. Chem. Eng. J. 314, 98–113. https://doi.org/10.1016/j.cej.2016.12.135.

CLU-IN, 1991. Dense nonaqueous Phase Liquids (dnapls). 2019. Clu-in.

Conte, L.O., Cotillas, S., Sánchez-Yepes, A., Lorenzo, D., Santos, A., 2022. LED visible light assisted photochemical oxidation of HCHs in aqueous phases polluted with DNAPL. Process Saf. Environ. Protect. 168, 434–442. https://doi.org/10.1016/j.psep.2022.10.015.

Demiray, Z., Akyol, N.H., Akyol, G., Copty, N.K., 2023. Surfactant-enhanced in-situ oxidation of DNAPL source zone: experiments and numerical modeling. J. Contam. Hydrol. 258. https://doi.org/10.1016/j.jconhyd.2023.104233.

Dominguez, C.M., Romero, A., Santos, A., 2019. Selective removal of chlorinated organic compounds from lindane wastes by combination of nonionic surfactant soil flushing and Fenton oxidation. Chem. Eng. J. 376. https://doi.org/10.1016/j.cej.2018.09.170.

Fernandez, J., Arjol, M.A., Cacho, C., 2013. POP-contaminated sites from HCH production in Sabinanigo, Spain. Environ. Sci. Pollut. Res. 20, 1937–1950. https://doi.org/10.1007/s11356-012-1433-8.

Fernández, J., Santos, A., Herranz, C., Cano, E., Lorenzo, D., Arjol, M.A., Salvatierra, A., 2023. LIFE SURFING PROJECT: surfactant enhanced chemical oxidation for remedia- ting DNAPL. In: Preparatory Work. 14th International HCH and Pesticides Forum, Zaragoza.

García-Cervilla, R., Romero, A., Santos, A., Lorenzo, D., 2020. Surfactant-enhanced solubilization of chlorinated organic compounds contained in dnapl from lindane waste: effect of surfactant type and ph. Int. J. Environ. Res. Public Health 17, 1–14. https://doi.org/10.3390/ijerph17124494.

Garcia-Cervilla, R., Santos, A., Romero, A., Lorenzo, D., 2021. Partition of a mixture of chlorina- ted organic compounds in real contaminated soils between soil and aqueous phase using surfactants: influence of pH and surfactant type. J. Environ. Chem. Eng. 9. https://doi.org/10.1016/j.jece.2021.105908.

García-Cervilla, R., Santos, A., Romero, A., Lorenzo, D., 2021. Compatibility of nonionic and anionic surfactants with persulfate activated by alkali in the abatement of chlorinated organic compounds in aqueous phase. Sci. Total Environ. 751. https://doi.org/10.1016/j.scitotenv.2020.141782.

Garcia-Cervilla, R., Santos, A., Romero, A., Lorenzo, D., 2022a. Abatement of chlorobenzenes in aqueous phase by persulfate activated by alkali enhanced by surfactant addition. J. Environ. Manage. 306. https://doi.org/10.1016/j.jenvman.2022.114475.

Garcia-Cervilla, R., Santos, A., Romero, A., Lorenzo, D., 2022b. Simultaneous addition of surfactant and oxidant to remediate a polluted soil with chlorinated organic compounds: slurry and column experiments. J. Environ. Chem. Eng. 10. https://doi.org/10.1016/j.jece.2022.107625.

Guadaño, J., Gómez, J., Fernández, J., Lorenzo, D., Domínguez, C.M., Cotillas, S., García-Cervilla, R., Santos, A., 2022. Remediation of the alluvial aquifer of the sardas landfill (Sabiñánigo, Huesca) by surfactant application. Sustainability (Switzerland) 14. https://doi.org/10.3390/su142416576.

Herzog, B.M., Kleinknecht, S.M., Haslauer, C.P., Klaas, N., 2023. Experimental upscaling analyses for a surfactant-enhanced in-situ chemical oxidation (S-ISCO) remediation design. J. Contam. Hydrol. 258. https://doi.org/10.1016/j.jconhyd.2023.104230.

Huo, L., Liu, G., Yang, X., Ahmad, Z., Zhong, H., 2020. Surfactant-enhanced aquifer remediation: mechanisms, influences, limitations and the countermeasures. Chemosphere 252, 126620. https://doi.org/10.1016/j.chemosphere.2020.126620.

Kang, S., Lim, H.S., Gao, Y., Kang, J., Jeong, H.Y., 2019. Evaluation of ethoxylated nonionic surfactants for solubilization of chlorinated organic phases: effects of partitioning loss and macroemulsion formation. J. Contam. Hydrol. 223. https://doi.org/10.1016/j.jconhyd.2019.03.007.

Liu, J.-W., Wei, K.-H., Xu, S.-W., Cui, J., Ma, J., Xiao, X.-L., Xi, B.-D., He, X.-S., 2021. Surfactant-enhanced remediation of oil-contaminated soil and groundwater: a review. Sci. Total Environ. 756, 144142 https://doi.org/10.1016/j.scitotenv.2020.144142.

Londergan, J., Yeh, L., 2003. Surfactant-Enhanced Aquifer Remediation (SEAR) Implementation Manual. INTERA INC AUSTIN TX.

Maire, J., Joubert, A., Kaifas, D., Invernizzi, T., Marduel, J., Colombano, S., Cazaux, D., Marion, C., Klein, P.Y., Dumestre, A., Fatin-Rouge, N., 2018. Assessment of flushing methods for the removal of heavy chlorinated compounds DNAPL in an alluvial aquifer. Sci. Total Environ. 612, 1149–1158. https://doi.org/10.1016/j.scitotenv.2017.08.309.

McCray, J.E., Tick, G.R., Jawitz, J.W., Gierke, J.S., Brusseau, M.L., Falta, R.W., Knox, R.C., Sabatini, D.A., Annable, M.D., Harwell, J.H., Wood, A.L., 2011. Remediation of NAPL source zones: lessons learned from field studies at hill and dover AFB. Ground Water 49, 727–744. https://doi.org/10.1111/j.1745-6584.2010.00783.x.

Mo, Y., Dong, J., Zhao, H., 2024. Field demonstration of in-situ microemulsion flushing for enhanced remediation of multiple chlorinated solvents contaminated aquifer. J. Hazard. Mater. 463. https://doi.org/10.1016/j.jhazmat.2023.132772.

Pennell, K.D., Capiro, N.L., Walker, D.I., 2014. Surfactant and cosolvent flushing. In: Kueper, B.H., Stroo, H.F., Vogel, C.M., Ward, C.H. (Eds.), Chlorinated Solvent Source Zone Remediation, 7, pp. 353–394.

Sáez, P., Santos, A., García-Cervilla, R., Romero, A., Lorenzo, D., 2022. Non-ionic surfactant recovery in surfactant enhancement aquifer remediation effluent with chlorobenzenes by semivolatile chlorinated organic compounds volatiliza- tion. Int. J. Environ. Res. Public Health 19. https://doi.org/10.3390/ijerph19127547.

Saint-Fort, R., 2022. Surfactants and their applications for remediation of hydrophobic organic contaminants in soils. IntechOpen. https://doi.org/10.5772/intechopen.100596.

Sánchez-Yepes, A., Santos, A., Romero, A., Lorenzo, D., 2024. Selective removal of chlorinated organic compounds from soil flushing emulsions: adsorbent regeneration with thermal-activated persulfate and surfactant recovery. J. Water Process Eng. 57. https://doi.org/10.1016/j.jwpe.2023.104644.

Santos, A., Fernández, J., Guadaño, J., Lorenzo, D., Romero, A., 2018a. Chlorinated organic compounds in liquid wastes (DNAPL) from lindane production dumped in landfills in Sabiñanigo (Spain). Environ. Pollut. 242, 1616–1624. https://doi.org/10.1016/j.envpol.2018.07.117.

Santos, A., Fernandez, J., Rodriguez, S., Dominguez, C.M., Lominchar, M.A., Lorenzo, D., Romero, A., 2018b. Abatement of chlorinated compounds in groundwater contaminated by HCH wastes using ISCO with alkali activated persulfate. Sci. Total Environ. 615, 1070–1077. https://doi.org/10.1016/j.scitotenv.2017.09.224.

Siegrist, R.L., Crimi, M., Simpkin, T.J., 2011. In Situ Chemical Oxidation for Groundwater Remediation, vol. 3. Springer Science & Business Media.

Stroo, H.F., Leeson, A., Marqusee, J.A., Johnson, P.C., Ward, C.H., Kavanaugh, M.C., Sale, T.C., Newell, C.J., Pennell, K.D., Lebrón, C.A., 2012. Chlorinated ethene source remediation: lessons learned. Environ. Sci. Technol. 46, 6438–6447. https://doi.org/10.1021/es204714w.

Sun, Y., Li, M., Gu, X., Danish, M., Shan, A., Ali, M., Qiu, Z., Sui, Q., Lyu, S., 2021. Mechanism of surfactant in trichloroethene degradation in aqueous solution by sodium persulfate activated with chelated-Fe(II). J. Hazard. Mater. 407 https://doi.org/10.1016/j.jhazmat.2020.124814.

Tomlinson, D.W., Rivett, M.O., Wealthall, G.P., Sweeney, R.E.H., 2017. Understanding complex LNAPL sites: illustrated handbook of LNAPL transport and fate in the subsurface. J. Environ. Manage. 204, 748–756. https://doi.org/10.1016/j.jenvman.2017.08.015.

Trellu, C., Mousset, E., Pechaud, Y., Huguenot, D., van Hullebusch, E.D., Esposito, G., Oturan, M.A., 2016. Removal of hydrophobic organic pollutants from soil washing/

flushing solutions: a critical review. J. Hazard. Mater. 306, 149–174. https://doi.org/10.1016/j.jhazmat.2015.12.008.

Tressler, A., Uchrin, C., 2014. Mathematical simulation of chlorinated ethene concentration rebound after in situ chemical oxidation. J. Environ. Sci. Health A Toxic/Hazard. Subst. Environ. Eng. 49, 869–881. https://doi.org/10.1080/10934529.2014.893790.

Vijgen, J., Abhilash, P., Li, Y.F., Lal, R., Forter, M., Torres, J., Singh, N., Yunus, M., Tian, C., Schäffer, A., 2011. Hexachlorocyclohexane (HCH) as new Stockholm convention POPs—a global perspective on the management of Lindane and its waste isomers. Environ. Sci. Pollut. Res. 18, 152–162. https://doi.org/10.1007/s11356-010-0417-9.

Vijgen, J., de Borst, B., Weber, R., Stobiecki, T., Forter, M., 2019. HCH and lindane contaminated sites: European and global need for a permanent solution for a long-time neglected issue. Environ. Pollut. 248, 696–705. https://doi.org/10.1016/j.envpol.2019.02.029.

Vijgen, J., Fokke, B., van de Coterlet, G., Amstaetter, K., Sancho, J., Bensaiah, C., Weber, R., 2022. European cooperation to tackle the legacies of hexachlorocyclohexane (HCH) and lindane. Emerg. Contam. 8, 97–112. https://doi.org/10.1016/j.emcon.2022.01.003.

Wang, Z., Yang, Z., Chen, Y.-F., 2023a. Pore-scale investigation of surfactant-enhanced DNAPL mobilization and solubilization. Chemosphere 341, 140071. https://doi.org/10.1016/j.chemosphere.2023.140071.

Wang, Z., Yang, Z., Hu, R., Chen, Y.-F., 2023b. Mass transfer during surfactant-enhanced DNAPL remediation: pore-scale experiments and new correlation. J. Hydrol. 621. https://doi.org/10.1016/j.jhydrol.2023.129586.

Wei, K.-H., Ma, J., Xi, B.-D., Yu, M.-D., Cui, J., Chen, B.-L., Li, Y., Gu, Q.-B., He, X.-S., 2022. Recent progress on in-situ chemical oxidation for the remediation of petroleum contaminated soil and groundwater. J. Hazard. Mater. 432, 128738 https://doi.org/10.1016/j.jhazmat.2022.128738.

Xu, Z., Cai, L., Zhou, Z., Yang, R., Zeng, G., Fu, R., Lyu, S., 2024. Surfactant enhanced persulfate system for the synergistic oxidation and reduction of mixed chlorinated hydrocarbons. J. Hazard. Mater. 469, 133887. https://doi.org/10.1016/j.jhazmat.2024.133887.